Journal of Translational Medicine

RESEARCH

Open Access

Lactate dehydrogenase A (LDHA)-mediated lactate generation promotes pulmonary vascular remodeling in pulmonary hypertension

Daiqian Wu[1†], Shuo Wang[2†], Fengxian Wang[2], Qing Zhang[3], Zhen Zhang[1*] and Xingbing Li[4*]

Abstract

Background High levels of lactate are positively associated with prognosis and mortality in pulmonary hypertension (PH). Lactate dehydrogenase A (LDHA) is a key enzyme for the production of lactate. This study is undertaken to investigate the role and molecular mechanisms of lactate and LDHA in PH.

Methods Lactate levels were measured by a lactate assay kit. LDHA expression and localization were detected by western blot and Immunofluorescence. Proliferation and migration were determined by CCK8, western blot, EdU assay and scratch-wound assay. The right heart catheterization and right heart ultrasound were measured to evaluate cardiopulmonary function.

Results In vitro, we found that lactate promoted proliferation and migration of pulmonary artery smooth muscle cells (PASMCs) in an LDHA-dependent manner. In vivo, we found that LDHA knockdown reduced lactate overaccumulation in the lungs of mice exposed to hypoxia. Furthermore, LDHA knockdown ameliorated hypoxia-induced vascular remodeling and right ventricular dysfunction. In addition, the activation of Akt signaling by hypoxia was suppressed by LDHA knockdown both in vivo and in vitro. The overexpression of Akt reversed the inhibitory effect of LDHA knockdown on proliferation in PASMCs under hypoxia. Finally, LDHA inhibitor attenuated vascular remodeling and right ventricular dysfunction in Sugen/hypoxia mouse PH model, Monocrotaline (MCT)-induced rat PH model and chronic hypoxia-induced mouse PH model.

Conclusions Thus, LDHA-mediated lactate production promotes pulmonary vascular remodeling in PH by activating Akt signaling pathway, suggesting the potential role of LDHA in regulating the metabolic reprogramming and vascular remodeling in PH.

Keywords Pulmonary hypertension, Lactate, Lactate dehydrogenase A, Vascular remodeling, Glycolysis

†Daiqian Wu and Shuo Wang equally contributed to this work.

*Correspondence:
Zhen Zhang
zhangzhen@swjtu.edu.cn
Xingbing Li
cqlxb1991@163.com

[1]Department of Cardiology, The Third People's Hospital of Chengdu, Affiliated Hospital of Southwest Jiaotong University, Chengdu Cardiovascular Disease Research Institute, Chengdu 610014, PR China
[2]Department of Cardiology, Daping Hospital, The Third Military Medical University, Chongqing 400042, PR China
[3]School of Pharmacy and Bioengineering, Chongqing University of Technology, Chongqing 400054, PR China
[4]Department of Cardiology, Chongqing Hospital of Traditional Chinese Medicine, Chongqing 400021, PR China

Introduction

Pulmonary hypertension (PH) is a chronic fatal disease characterized by vascular remodeling and increased pulmonary artery resistance, principally manifesting as the progressive proliferation of pulmonary artery smooth muscle cells (PASMCs) [1]. Current treatments can improve the symptoms and hemodynamic parameters of PH, but cannot reverse vascular remodeling and do not significantly reduce morbidity and mortality [2]. Therefore, new methods to treat PH are urgently needed.

Metabolic disorders exist in the development of PH, and glycolysis, or the Warburg effect, is the key mechanism for the development of PH [3]. This metabolic shift favors lactate formation [4]. Multiple studies have confirmed that there is significant glycolysis and excessive proliferation in PASMCs from PH patients or animal models [5, 6]. The latest research shows that hyperlactic acidemia is an independent predicting factor for mortality in PH patients [7]. Previously, lactate was merely thought to be metabolic waste. However, an increasing number of studies have shown that lactate can also serve as a signaling molecule, participating in glucose metabolism, fat synthesis and the post-translational modification of proteins [8–10]. Recent studies have shown that lactate plays a key role in processes such as proliferation, cell cycle progression and apoptosis [11–13]. Although some studies have confirmed that some key enzymes in glycolysis promote both glycolysis and the proliferation of PASMCs, how glycolysis itself promotes the proliferation of PASMCs still requires further study.

Lactate dehydrogenase A (LDHA) is encoded by the *LDHA* gene and usually exists as a tetramer. LDHA contains 332 amino acids and forms a double-leaf structure [14]. The main function of LDHA is to convert pyruvate to lactate and NADH to NAD+ [15]. LDHA is primarily located in the cytoplasm, but LDHA is also found in the mitochondria and nuclei. In the cytoplasm, LDHA plays a key role in glycolysis, whereas in the nucleus, LDHA functions as a single-stranded DNA-binding protein and may be involved in DNA replication and transcription [16]. Studies have shown that LDHA is highly expressed in a variety of tumors, promoting tumor cell proliferation and metastasis through the production of lactate [17, 18]. The latest research shows that LDHA plays an important role in cardiac hypertrophy, heart failure and myocardial damage [19–21]. More importantly, the levels of LDHA in the plasma of patients with PH were found to be significantly increased, suggesting an association between LDHA and PH risk [22]. However, the effect of LDHA on the development of PH remains unclear.

In this study, we demonstrated that lactate levels and LDHA expression were increased in the lung tissue of mice with hypoxia-induced PH. Lactate promoted the proliferation and migration of PASMCs, and LDHA knockdown inhibited the proliferation and migration of PASMCs induced by hypoxia. The effects above may be achieved through the activation of Akt. More importantly, our data demonstrated that LDHA knockdown and LDHA inhibitors alleviated pulmonary artery pressure and vascular remodeling in PH animal models. These results suggest that LDHA may be a new target for PH treatment.

Materials and methods

Animal models

C57BL/6J male mice (Age: 6–8 weeks; Weight: 20–25 g) and male Sprague-Dawley rats (190–200 g) were purchased from Charles River (Beijing, China). To minimize experimental variability, only male animals were chosen for the study. While women are generally more susceptible to PH than men, most animal studies have indicated that female sex and estrogen supplementation exert a protective effect against PH [23–25]. All experimental animal procedures were performed in accordance with the Guide for the Care and Use of Laboratory Animals published by the US National Institutes of Health (NIH publication no. 85–23, revised 1996) and were approved by the Animal Care and Use Committee of the Third Military Medical University (Approval number: AMUWEC20201184).

We used the hypoxic PH mouse model to study the role of LDHA/lactate in PH. Mice were randomly exposed to normoxia (21% O_2) or hypoxia (10% O_2) for 4 weeks as previously described ($n=6$) [26]. Briefly, the mice were housed in a chamber (AIPUINS, Hangzhou, China) with a mixture of oxygen and nitrogen. For the LDHA knockdown studies ($n=6$), mice were delivered with 1×10^{11} genome copies of either AAV9-shLDHA or AAV9-NC (Shanghai Genechem Co., Ltd) via tail vein in a final solution of 100 μL 7 days before being exposure to normoxia or hypoxia. After 4 weeks of hypoxia, right heart catheterization and echocardiography were performed, then mice were sacrificed for analysis.

We used hypoxic PH models ($n=6$), Sugen/hypoxia (SuHx) PH models ($n=6$) and Monocrotaline (MCT) PH models ($n=6$) to study the therapeutic effect of LDHA inhibitor (GSK2837808A, 6 mg/kg/day, HY-N0643, MedChemExpress, USA) on PH. Dosage of LDHA inhibitors was based on previous studies [27]. For SuHx PH mice model, mice were either injected with SU5416 (20 mg/kg, HY-10374, MedChemExpress, USA) or vehicle weekly by subcutaneous injection, exposed to hypoxia conditions for 3 weeks (10% O_2) and returned to normoxia (21% O_2) for 2 weeks. Normoxic controls were kept in room air only (21% O_2) for a total of 5 weeks. Mice were also randomly assigned to four different experimental groups: (i) normoxia for 5 weeks, (ii) normoxia for 3 weeks + GSK2837808A/normoxia for 2 weeks, (iii)

SuHx for 3 weeks + normoxia for 2 weeks, (iv) SuHx for 3 weeks + GSK2837808A/normoxia for 2 weeks. For MCT-induced PH rat model, a single subcutaneous injection MCT (60 mg/kg, HY-N0750, MedChemExpress, USA) or sterile saline was given to male Sprague-Dawley rats to develop PH. Rats were also randomly assigned to four different experimental groups: (i) control for 3 weeks + saline for 2 weeks, (ii) control for 3 weeks + GSK2837808A for 2 weeks, (iii) MCT for 3 weeks + saline for 2 weeks, (iv) MCT for 3 weeks + GSK2837808A for 2 weeks. At the end of the fifth week, right heart catheterization and echocardiography were performed, then mice or rats were sacrificed for analysis.

Rodent echocardiography

Right ventricle functions of the PH models were assessed by functional rodent echocardiography according to the procedures described previously [28]. Briefly, animals were anesthetized by inhalation of isoflurane, and then cardiac function parameters were detected. Color Doppler was used to record pulmonary blood flow at the level of the aortic valve in the short-axis view to measure pulmonary acceleration time (PAT) and pulmonary ejection time (PET). Tricuspid annular plane systolic excursion (TAPSE) was measured by using two-dimensional M-mode echocardiography in the apical 4-chamber view to find the lateral tricuspid annulus of the free right ventricular (RV) wall. Right ventricular fractional area change (RVFAC) was measured at the level of the midnipple through the parasternal short-axis view. Right ventricular free wall thickness (RVFWT) was measured at end-diastole in two-dimensional parasternal short-axis mitral valve level or in M-mode at the parasternal long-axis RV outflow tract level.

Analysis of RVSP and Fulton index

Right ventricular systolic pressure (RVSP) was measured through the external carotid vein using a polyethylene-50 catheter with a BL-420 S biological function experimental system (Chengdu Techman, China). Briefly, following abdominal anesthesia of mice/rats, a skin incision was made from the mandibles to sternum. Careful dissection was performed to expose the right jugular vein and trachea. Two pieces of suture were placed on top of the right jugular vein. The suture closest to the mandibles was tied to restrict blood flow to a tiny trickle, while the suture nearest to the sternum was loosely knotted around the vein. A hole was then created between the two sutures using micro-scissors, and the polyethylene catheter connected to the baroreceptor was inserted into the right ventricle. RVSP was continuously monitored for 5–10 min. After RVSP measurement, mice were euthanized and blood, lungs, and hearts were collected. The RV, left ventricle (LV), and interventricular septum (S) were dissected and weighed. The RV/(LV + S) ratio, known as the Fulton index, was calculated as an indicator of right ventricular hypertrophy.

Hematoxylin-eosin (H&E) staining and Elastica Van Gieson (EVG) staining

Briefly, lung tissue samples were stored in 4% paraformaldehyde for 24 h, then embedded in paraffin, sectioned, placed on glass slides, dewaxing and re-hydrating with xylene and ethanol of different concentrations. For H&E staining, the sections were processed by the following steps: staining with hematoxylin (G1120, Solarbio) solution for 20 s, rinsing with running water for 5 min, soaking in 1% acid alcohol for 5 s, and counterstaining with eosin Y solution (G1120, Solarbio) for 1 min. For EVG staining, the Collagen Fiber And Elastic Fiber Staining Kit (G1597, Solarbio) was applied. Briefly, the slides were stained with modified VG Staining Solution for 10 min, washed with distilled water for 10 s, stained with Vehoeff Working Solution for 5 min and washed with water, then subjected to Vehoeff Differentiation Solution for 30 s, until the elastic fibers were clear.

Immunofluorescence staining

The specific operation was described previously [29]. Briefly, lung tissues were fixed in 4% formaldehyde and permeabilized with 0.25% TritonX-100. Next, samples were blocked with Blocking Buffer (P0260, Beyotime) and washed 5 times with PBS. Lung tissue incubated with the corresponding primary antibodies ((1:100, α-SMA, ab21027, abcam); (1:100, LDHA, 3582, Cell Signaling Technology); (1:100, Ki67, 34330, Cell Signaling Technology) overnight at 4 °C. Then, tissue sections were added with the appropriate fluorescence-conjugated secondary antibodies (SA00009-2, Proteintech; SA00003-1, Proteintech). Images were scanned with a confocal microscope (Olympus, Tokyo, Japan).

Cell culture and treatment

Mice pulmonary artery smooth muscle cells (mPASMCs, CP-M002, China) were provided by Procell Life Science&Technology Co.,Ltd. mPASMCs were cultured in Cell Medium (CM-M002, Procell Life Science&Technology Co.,Ltd, China) at 37 °C with 5% carbon dioxide. To investigate the effects of lactate on mPASMCs, cells were exposed to lactate (concentration gradient 0–20 mM, Sigma-Aldrich) for 24 h. To examine the effect of LDHA on mPASMCs under normoxic or hypoxic conditions, mPASMCs were transfected with LDHA siRNA (100 nM, sc-43893, Santa Cruz). To activate Akt signaling pathway, the Akt overexpression plasmid (Shanghai Genechem Co., Ltd) was transfected into cells using Lipofectamine 3000 (#L3000008, Invitrogen, United States) according to the

manufacturer's instructions. Briefly, when mPASMCs reached a 70–80% confluent, 2500 ng plasmid, 200 μL Opti-MEM (#31985070, Thermo Fisher Scientific), 5 μL P3000 reagent, and 5 μL lipofectamine reagent were used to prepare the DNA-plasmid complexes. After a 15-minute incubation, the complexes were directly added to the culture. After 24 h of transfection, the cells were placed in a hypoxia workstation with 2% O_2 or a normal cell incubator with 21% O_2 for another 24 h before conducting subsequent assays.

Cell proliferation, cell viability

Cell viability was measured by CCK8 assays. Briefly, mPASMCs were seeded in 96-well plates and treated as mentioned above. Then, cells were incubated with CCK8 solution (C0037, Beyotime) for 2 h, and the OD value was measured using a microplate reader at 450 nm. Cell proliferation was determined by the EdU incorporation assay. In brief, after treatment described in the previous section, cells were cultured in the presence of EdU (10 μM) for another 2 h and then staining using Click-iT™ EdU Cell Proliferation Kit (C0071S, Beyotime) according to the manufacturer's instructions. Images were acquired by confocal microscope and quantified using Image J (NIH, Bethesda, MD).

Scratch test

Scratch test was performed as previously described [30]. Briefly, use a 100 μL pipette tip to draw regular "cross"-shaped cell scars on each set of culture dishes and take photos. Observe and take pictures every 24 h. Migration was quantified as percent scratch area using Image J software.

Lactate measurement

The lactate levels in cell supernatants, serum or lung tissues were measured by a lactate assay kit (ab65330, abcam) according to the manufacturer's instructions. For detection in cell samples, mPASMCs were cultured in 6-well plates and treated as described above, the cell supernatants were collected for subsequent measurement. For detection in serum or lung tissues, samples were harvested from hypoxic PH models after 4 weeks of exposure to normoxia or hypoxia.

Cell supernatants or serum were deproteinized using a 10 kD Spin column (ab93349, abcam) to eliminate high amount of proteins. Endogenous LDH enzymes in lung tissues were removed utilizing the Deproteinizing Sample Preparation Kit (ab204708, abcam). Following a 30-minute incubation with the reaction mix, the OD value was assessed using a microplate reader at 570 nm.

Western blotting

Total proteins were isolated from the lung tissues or cells. 20 mg of each lung specimen was lysed with RIPA buffer containing PMSF (Solarbio). Protein concentration was determined by BCA protein assay kit (Beyotime), and protein samples (20–30 μg/lane) were electrophoresed and transferred to nitrocellulose filters (Millipore Sigma). Image J was used to analyze the average gray value of each band. The primary antibodies in this study were as follows: anti-β-actin (1:500; SC-130657, Santa Cruz), anti-LDHA (1:1000; 3582, Cell Signaling Technology), anti-Akt (1:1000; 60203-2-Ig, Proteintech), anti-pAkt (1:1000; 80455-1-RR, Proteintech), anti-PCNA (1:1000; 13110, Cell Signaling Technology), anti-Cyclin D1 (1:100; sc-8396, Santa Cruz).

Statistical analysis

All data were represented as mean ± SD. GraphPad Prism 7.0 was used to perform the statistical analysis. Student's unpaired t-test was used to compare two independent groups. In experiments comparing multiple time points, t-tests were used for each time point. A value of $P<0.05$ was considered significant.

Results

Hypoxia increased the levels of lactate and LDHA expression in the hypoxia-induced PH mouse model

In order to explore the role of lactate in PH, we constructed a hypoxic PH model. Hypoxia increased the RVSP (Fig. 1A1, A2) and the ratio of the right ventricle/left ventricle plus septum (Fulton index) (Fig. 1B). In addition, hypoxia increased the lactate content in the plasma and lung tissue of the PH model (Fig. 1C). LDHA serves as the pivotal enzyme in lactate production. We found that hypoxia significantly increased the expression of LDHA in lung tissue (Fig. 1D1, D2), with notably high LDHA expression levels observed in PASMCs from the PH model (Fig. 1E). Since LDHA knockout is lethal in mice [31], we used AAV9-shLDHA to knockdown LDHA in vascular smooth muscle cells (Additional file 1: Figure S1). The results showed that lactate levels in plasma and lung tissue were significantly reduced by AAV9-shLDHA under hypoxia (Fig. 1F).

The results above indicate that LDHA promotes lactate production in a hypoxia-induced PH mouse model.

Lactate promoted the proliferation and migration of mPASMCs in an LDHA-dependent manner

The effects of lactate were then examined in vitro. The abnormal proliferation and migration of PASMCs are important mechanisms of vascular remodeling in PH [1]. Based on the lactate content in the mice with hypoxia-induced PH, we set a lactate concentration gradient (0–20 mM). The results of the CCK8 assays (Fig. 2A) and

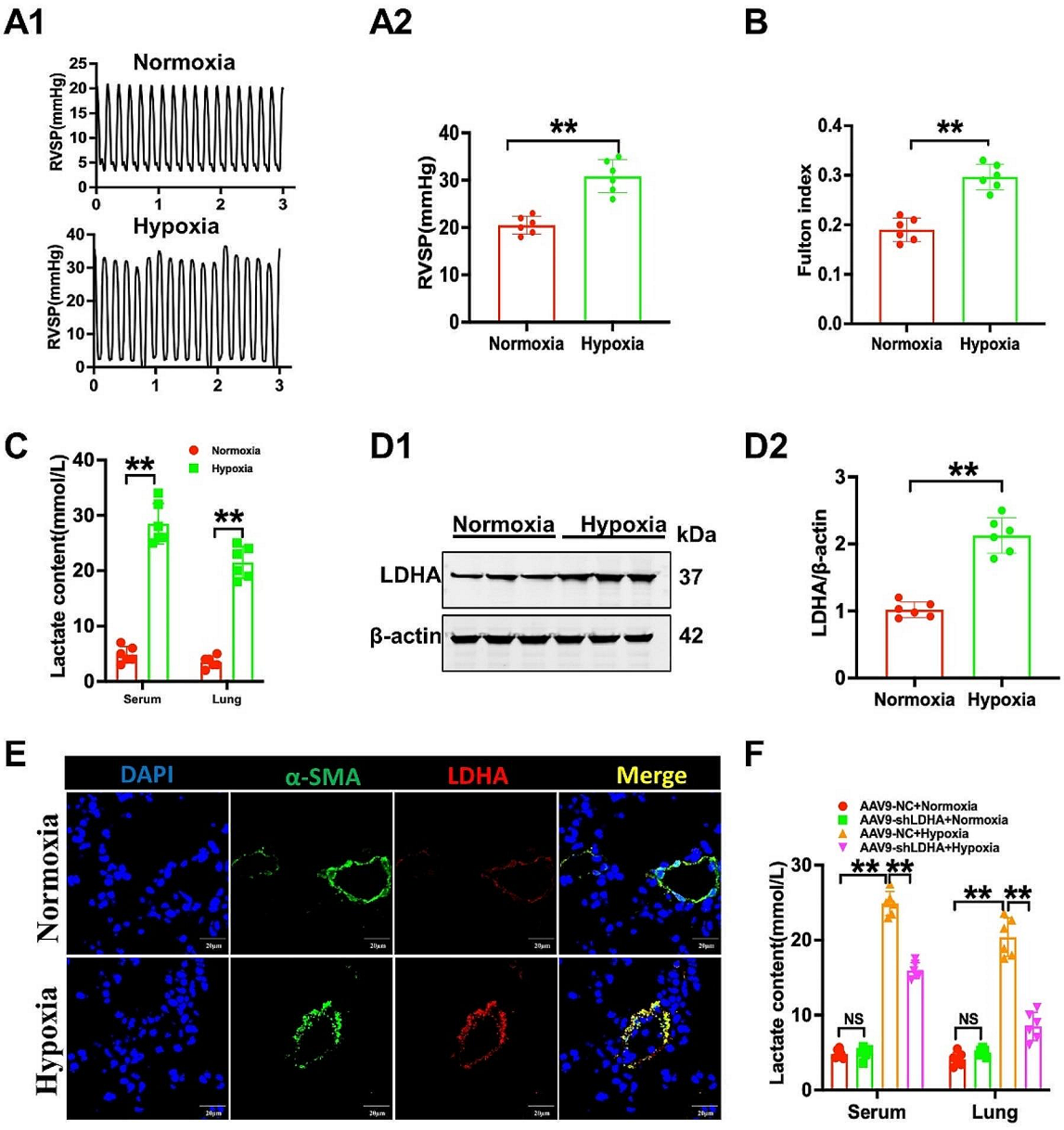

Fig. 1 Hypoxia increased the levels of lactate and LDHA expression in hypoxia-induced PH mouse model. (**A and B**) The RVSP (**A**) and Fulton index (**B**) were determined in mice exposed to normoxia or hypoxia for 4 weeks. (**C**) Lactate levels in plasma and lung tissues were measured in mice exposed to either normoxia or hypoxia for 4 weeks. (**D**) Western blots (D1) and quantitative data (D2) of LDHA protein expression of lung tissue in experimental groups. (**E**) Representative images of mouse lung tissue sections were subjected to fluorescence staining of α-SMA (green) and LDHA (red) after 4 weeks of exposure to either normoxia or hypoxia. DAPI were utilized to stain cell nuclei (blue). (**F**) Lactate levels in mouse plasma and lung tissues of each group. Data were presented as Mean ± SD. $n = 6$, NS: no statistical signification, $^{**}p < 0.01$

EdU staining (Fig. 2B1, B2) suggested that lactate could promote the proliferation of mPASMCs in a concentration-dependent manner. The protein levels of cyclin D1 and PCNA in mPASMCs were upregulated by lactate (Fig. 2C). Furthermore, we found that lactate promoted mPASMCs migration (Fig. 2D1, D2). Interestingly, the increases in the lactate levels of mPASMCs supernatants exposed to hypoxia were downregulated by LDHA knockdown (Fig. 2E). In addition, the results of the CCK8 assays (Fig. 2F) and EdU staining (Fig. 2G1, G2) showed

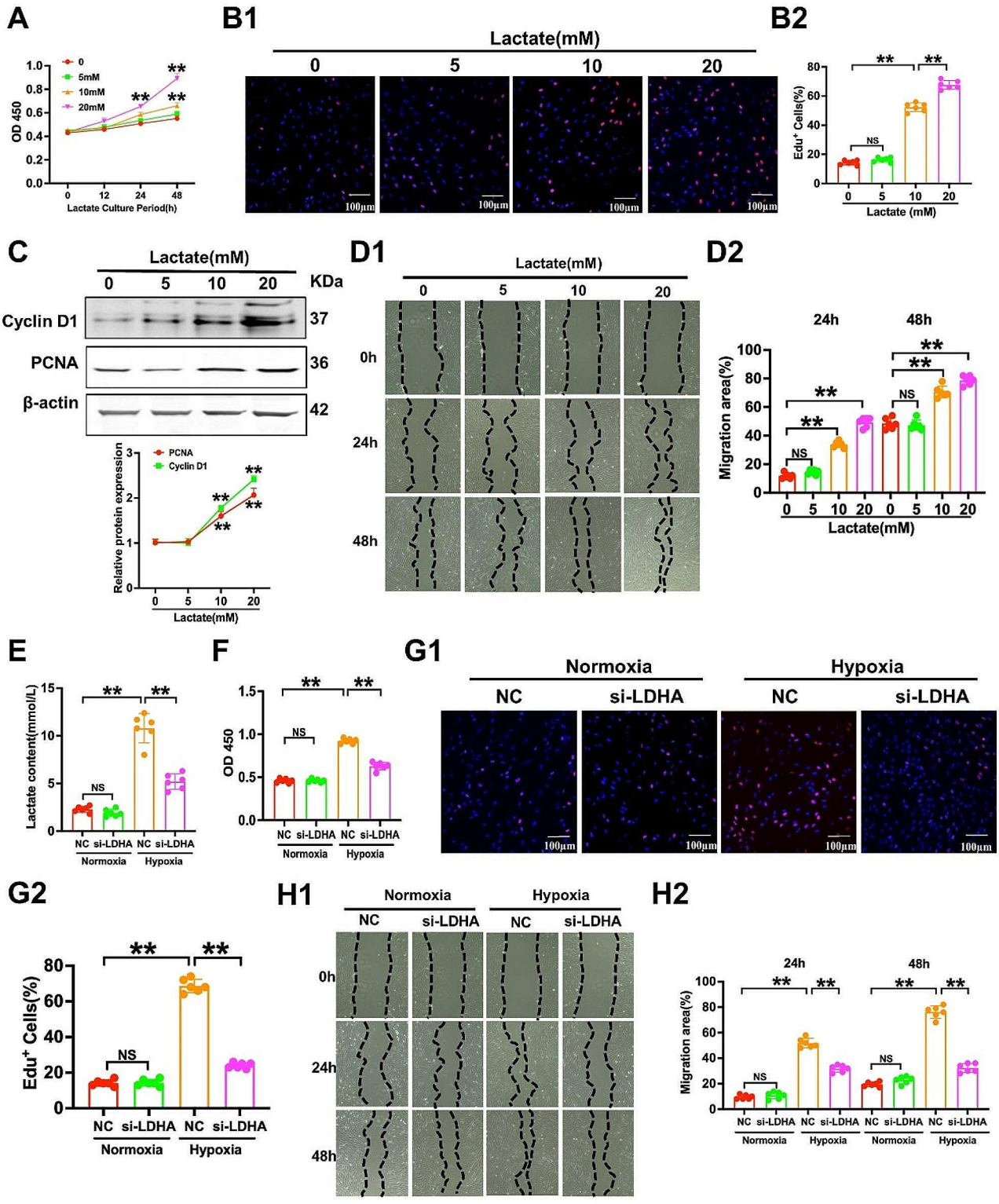

Fig. 2 (See legend on next page.)

(See figure on previous page.)

Fig. 2 Lactate promoted proliferation and migration of mPASMCs in an LDHA-dependent manner under hypoxia. (**A**) The effect on mPASMCs viability was assessed using the CCK-8 assay after treatment with lactate for 0, 24 and 48 h at various concentrations (0, 5, 10, and 20 mM). (**B**) The impact of lactate-induced mPASMC proliferation at different concentrations (0, 5, 10, and 20 mM) was evaluated following 24 h of lactate treatment using the EdU incorporation assay. Representative images (**B1**) and quantification (**B2**) of the EdU assay in mPASMCs were presented. (**C**) Representative images of Western blots and the combined quantitative data (below) show the expression of PCNA and Cyclin D1 in mPASMCs after treatment with lactate for 24 h at different concentrations (0, 5, 10, and 20 mM). (**D**) Representative images (**D1**) of the wound healing assay of mPASMCs in vitro and quantification (**D2**) of the wound healing assay of mPASMCs after treatment with lactate for 0, 24 and 48 h at different concentrations (0, 5, 10, and 20 mM). (**E**) Lactate levels in the cell supernatants of mPASMCs were measured for each group. (**F**) The viability of mPASMCs in each group was evaluated using the CCK-8 assay. (**G**) The impact of LDHA on mPASMCs proliferation under normoxia or hypoxia was evaluated using the EdU incorporation assay, as depicted in representative images (**G1**) and quantification (**G2**) of the EdU assay of mPASMCs. (**H**) The Effect of LDHA on mPASMCs migration was measured by wound healing assay under normoxia or hypoxia, shown in representative images (**H1**) and quantification data (**H2**). Data were presented as Mean ± SD. $n = 4–6$, NS: no statistical signification, $^{**}p < 0.01$

that the hyperproliferation of mPASMCs exposed to hypoxia was inhibited by LDHA knockdown. Furthermore, hypoxia promoted the migration of mPASMCs, but LDHA knockdown reversed this effect (Fig. 2H1, H2).

Taken together, the in vitro results suggest that lactate promotes the proliferation and migration of PASMCs in an LDHA-dependent manner under hypoxia.

LDHA knockdown reduced pulmonary artery pressure and improved pulmonary artery vascular remodeling

AAV9 vectors for LDHA knockdown were used to study the role of LDHA in PH. Our results showed that LDHA knockdown decreased RVSP (Fig. 3A1, 3A2) and Fulton index (Fig. 3B). Furthermore, the parameters of the right ventricular function such as PAT/PET (Fig. 3C), TAPSE (Fig. 3D) and RVFAC% (Fig. 3E) were increased by LDHA knockdown in mice with hypoxic pulmonary hypertension. Right ventricular hypertrophy (Fig. 3F) and pulmonary arterial wall thickening (Fig. 3G1, G2) were attenuated by LDHA knockdown in mice exposed to hypoxia.

Taken together, these results suggest that LDHA contributes to the development of pulmonary hypertension by promoting pulmonary artery vascular remodeling.

LDHA knockdown reduced the hyperproliferation of PASMCs in mice with hypoxia-induced pulmonary hypertension

PASMCs hyperproliferation is a central mechanism of vascular remodeling in PH [1]. Similar to the in vitro results, the findings revealed that hypoxia led to an increase in PCNA, cyclin D1 and p-Akt protein levels in lung tissue, as well as the fact that LDHA knockdown reverses this effect (Fig. 4A1-A4). The results of the Ki67 staining showed that hypoxia-induced PASMCs hyperproliferation was inhibited by LDHA knockdown in vivo (Fig. 4B1, B2).

Taken together, these data suggest that LDHA promotes PASMCs hyperproliferation in mice exposed to hypoxia.

LDHA promoted the proliferation and migration of PASMCs exposed to hypoxia via Akt

Previous studies have shown that an LDHA deficiency impairs the Akt signaling pathway [32]. Consistent with the in vivo results, we demonstrated that the knockdown of LDHA inactivated Akt signaling in mPASMCs exposed to hypoxia (Fig. 5A1-A3). An Akt overexpression plasmid was used to explore the underlying mechanism. The results indicated that the inhibitory effect of LDHA knockdown on proliferation in hypoxia-induced mPASMCs was reversed by Akt (Fig. 5B1, B2). Furthermore, the results showed that the inhibitory effect of LDHA knockdown on proliferation (Fig. 5C1, C2) and migration (Fig. 5D1, D2) in hypoxia-induced mPASMCs was reversed by Akt.

Taken together, these results suggest that LDHA activates Akt signaling to promote hyperproliferation in PASMCs exposed to hypoxia.

The therapeutic effects of an LDHA inhibitor in Sugen/hypoxia-induced pulmonary hypertension

We then selected an LDHA inhibitor in order to elucidate its potential therapeutic effects. As shown in Fig. 6A, mice were treated with Sugen/hypoxia for 3 weeks, followed by an administration of the LDHA inhibitor under normoxia for 2 weeks. Our results showed that the LDHA inhibitor decreased RVSP (Fig. 6B1, B2) and Fulton index (Fig. 6C). Furthermore, TAPSE (Fig. 6D) was increased by the LDHA inhibitor. Right ventricular hypertrophy (Fig. 6E) and pulmonary arterial wall thickening (Fig. 6F1, F2) were attenuated by the LDHA inhibitor in mice exposed to Sugen/hypoxia. From a mechanistic perspective, the LDHA inhibitor reversed the increase in PCNA, cyclin D1 and p-Akt protein levels in this PH model (Fig. 6G1-G4).

In conclusion, the results above suggest that LDHA inhibitors have a therapeutic role in Sugen/hypoxia-induced PH via inhibiting Akt signaling pathway.

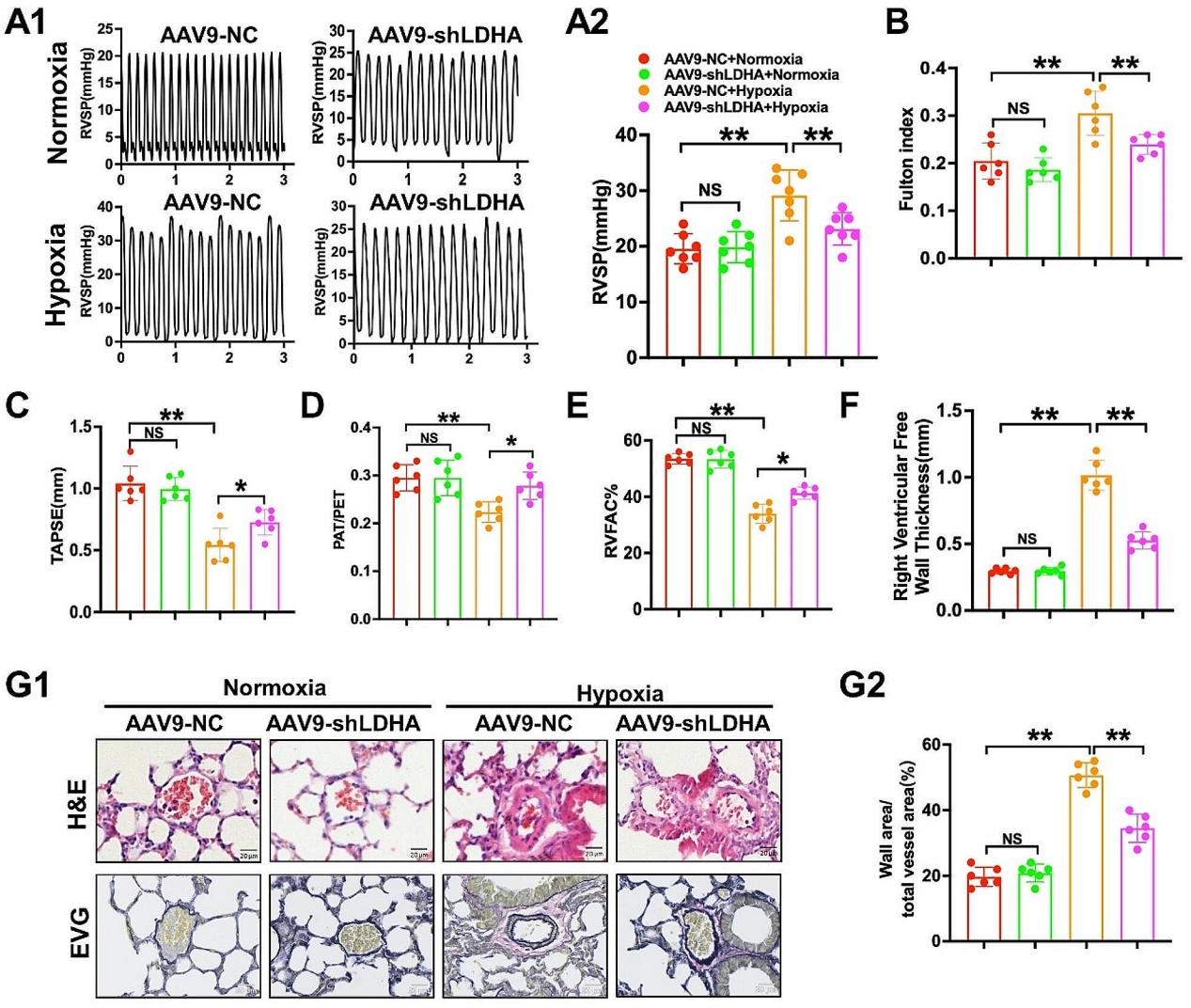

Fig. 3 LDHA knockdown reduces pulmonary artery pressure and improves pulmonary artery vascular remodeling. (**A and B**) The RVSP (**A1, A2**) and Fulton index (**B**) were determined in experimental mice exposed to normoxia or hypoxia for 4 weeks. (**C to F**) Quantification of TAPSE (**C**), PAT/PET (**D**), RVFAC% (**E**), and RVFWT (**F**) was performed after 4 weeks of normoxia or hypoxia in experimental mice injected with AAV9-shLDHA or AAV9-NC via the tail vein. (**G**) Representative histological images of lung sections stained with H&E and Elastica van Gieson (EVG) in each experimental group (**G1**). The wall thickness of the pulmonary arteries was measured (**G2**). TAPSE, Tricuspid Annular Plane Systolic Excursion; PAT, Pulmonary Acceleration Time; PET, Pulmonary Ejection Time. RVFAC, Right Ventricular Fractional Area Change. RVFWT, Right Ventricular Free Wall Thickness. Data were presented as Mean ± SD. $n = 6$, NS: no statistical signification, $^{*}p < 0.05$, $^{**}p < 0.01$

The therapeutic effects of an LDHA inhibitor in MCT-induced pulmonary hypertension

Then, the effects of an LDHA inhibitor in MCT-induced PH were examined. As shown in Fig. 7A, rats were treated with MCT for 3 weeks, followed by administration of an LDHA inhibitor for 2 weeks. Our results showed that the LDHA inhibitor decreased RVSP (Fig. 7B1, B2) and Fulton index (Fig. 7C). Furthermore, TAPSE was increased by the LDHA inhibitor (Fig. 7D). Right ventricular hypertrophy (Fig. 7E) and pulmonary arterial wall thickening (Fig. 7F1, F2) were reduced by LDHA inhibition in rats treated with MCT. Mechanistically, the LDHA inhibitor also reversed the increase in PCNA, cyclin D1 and p-Akt protein levels in rat PH model (Fig. 7G1-G4).

In conclusion, the results above suggest that LDHA inhibitors have a therapeutic role in MCT-induced PH via inhibiting Akt signaling pathway.

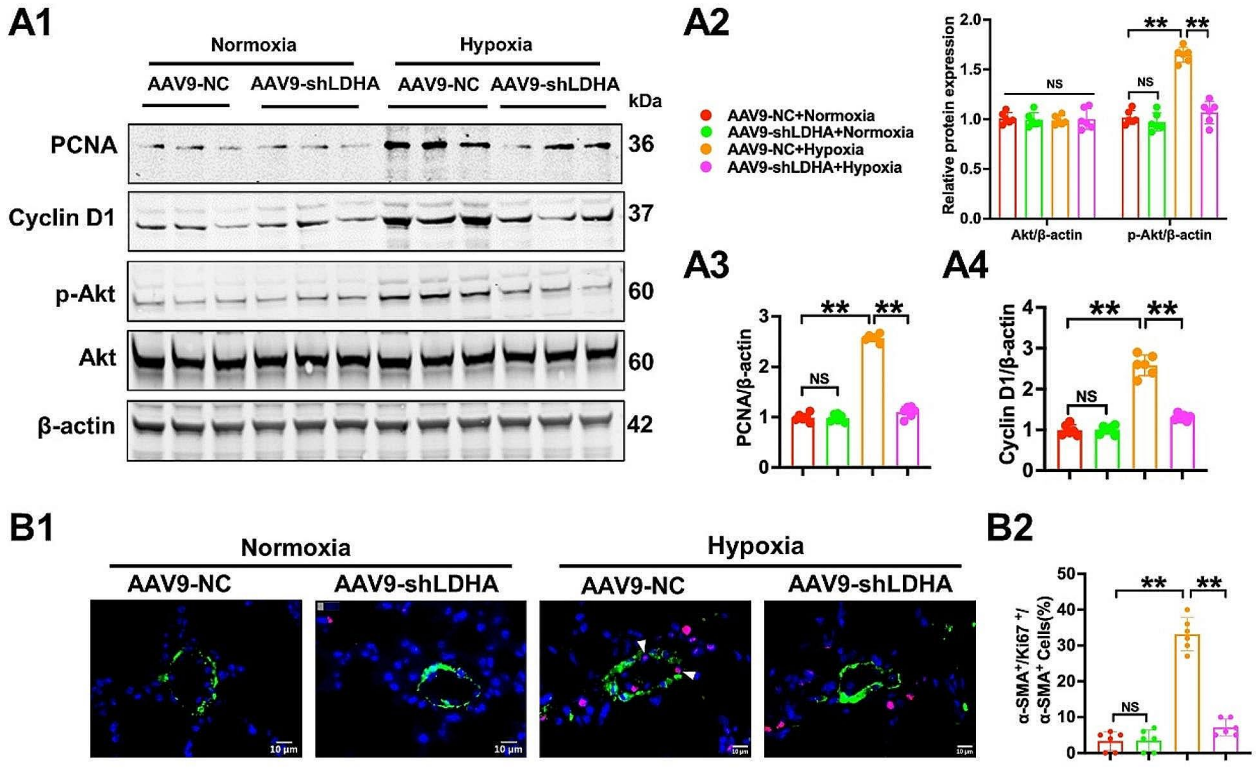

Fig. 4 LDHA knockdown reduced hyperproliferation of PASMCs in mice with hypoxia-induced pulmonary hypertension. (**A**) Representative images of Western blots (A1) and the combined quantitative data show the expression of p-Akt, Akt (A2), PCNA (A3), Cyclin D1 (A4) of lung tissue in experimental groups. (**B**) Representative images (B1) of mouse lung tissue sections were subjected to fluorescence staining of α-SMA (green) and Ki67 (red) in experimental groups. DAPI were utilized to stain cell nuclei (blue). The percentage of Ki67 + cells in PASMCs was quantified (B2). Data were presented as Mean ± SD. $n = 6$, NS: no statistical signification, $^{**}p < 0.01$

The therapeutic effects of an LDHA inhibitor in chronic hypoxia-induced mouse pulmonary hypertension

Finally, we examined the potential therapeutic effects of an LDHA inhibitor on chronic hypoxia-induced mouse PH models. As depicted in Fig. 8A, mice were subjected to hypoxia for 4 weeks and treated with GSK2837808A throughout this period. Our results demonstrate that the LDHA inhibitor reduced RVSP (Fig. 8B1, B2) and Fulton index (Fig. 8C), while increasing TAPSE (Fig. 8D). Additionally, the LDHA inhibitor attenuated right ventricular hypertrophy (Fig. 8E) and pulmonary arterial wall thickening (Fig. 8F1, F2) in mice exposed to chronic hypoxia.

In summary, these findings suggest that LDHA inhibitors hold therapeutic potential for chronic hypoxia-induced mouse PH.

Discussion

Vascular remodeling is a typical feature of PH, and glycolysis is an important mechanism that promotes the proliferation and migration of PASMCs [3]. However, the role and mechanism of lactate, an end product of glycolysis, in vascular remodeling remains unclear. In this study, we investigated the role and mechanism of lactate in pulmonary artery vascular remodeling. The principal findings were as follows: (1) there was an increase in lactate levels and LDHA expression in the lung tissue of mice with hypoxic PH, and lactate promoted PASMC proliferation and migration; (2) LDHA knockdown reduced the lactate levels in plasma and lung tissue and inhibited hypoxia-induced PASMCs proliferation and migration; (3) LDHA knockdown reduced pulmonary artery pressure and improved right ventricle function by reducing vascular remodeling; (4) a possible mechanism could be that lactate activated Akt to promote PASMCs proliferation and migration; and (5) the LDHA inhibitor had a therapeutic effect in multiple PH models.

Increasing evidence emphasizes the important role of lactate in cardiovascular diseases [33–35]. The latest research indicates that lactate promotes the change in vascular smooth muscle cells to a synthetic phenotype

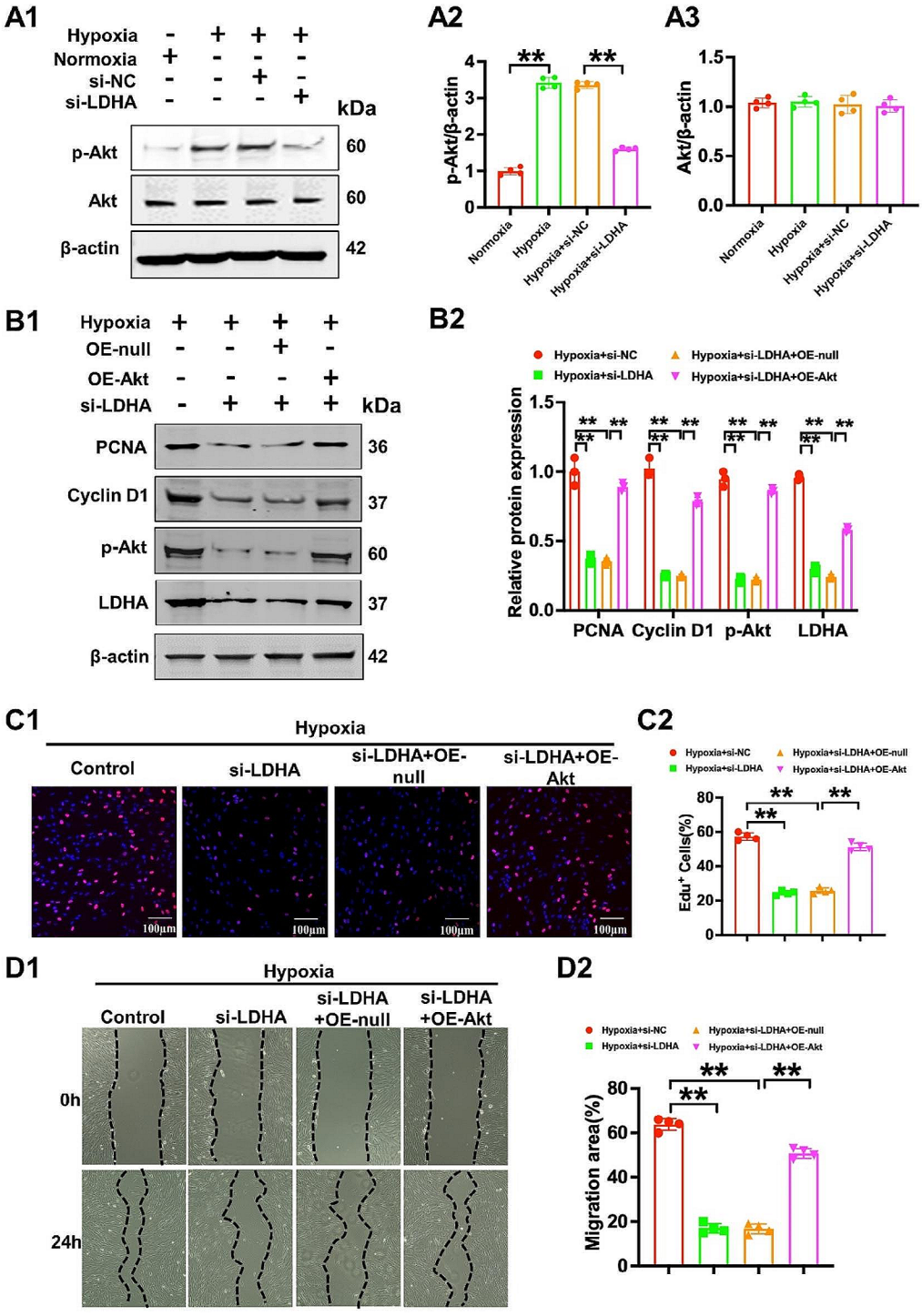

Fig. 5 LDHA promoted proliferation and migration of mPASMCs exposed to hypoxia via Akt. (**A**) Representative images of Western blots (A1) and the combined quantitative data show the expression of p-Akt (A2) and Akt (A3) in mPASMCs. (**B**) Representative images of Western blots (B1) and the combined quantitative data show the expression of p-Akt, LDHA, PCNA and Cyclin D1 (B2) in mPASMCs. (**C**) The effect of Akt on LDHA-mediated cell viability under hypoxia detected by EdU assay, shown in representative images (C1) and quantification data (C2). (**D**) Representative images (D1) of the wound healing assay of mPASMCs in vitro and quantification of the wound healing assay of mPASMCs (D2). Data were presented as Mean ± SD. $n = 3–4$, NS: no statistical signification, $^{*}p < 0.05$, $^{**}p < 0.01$

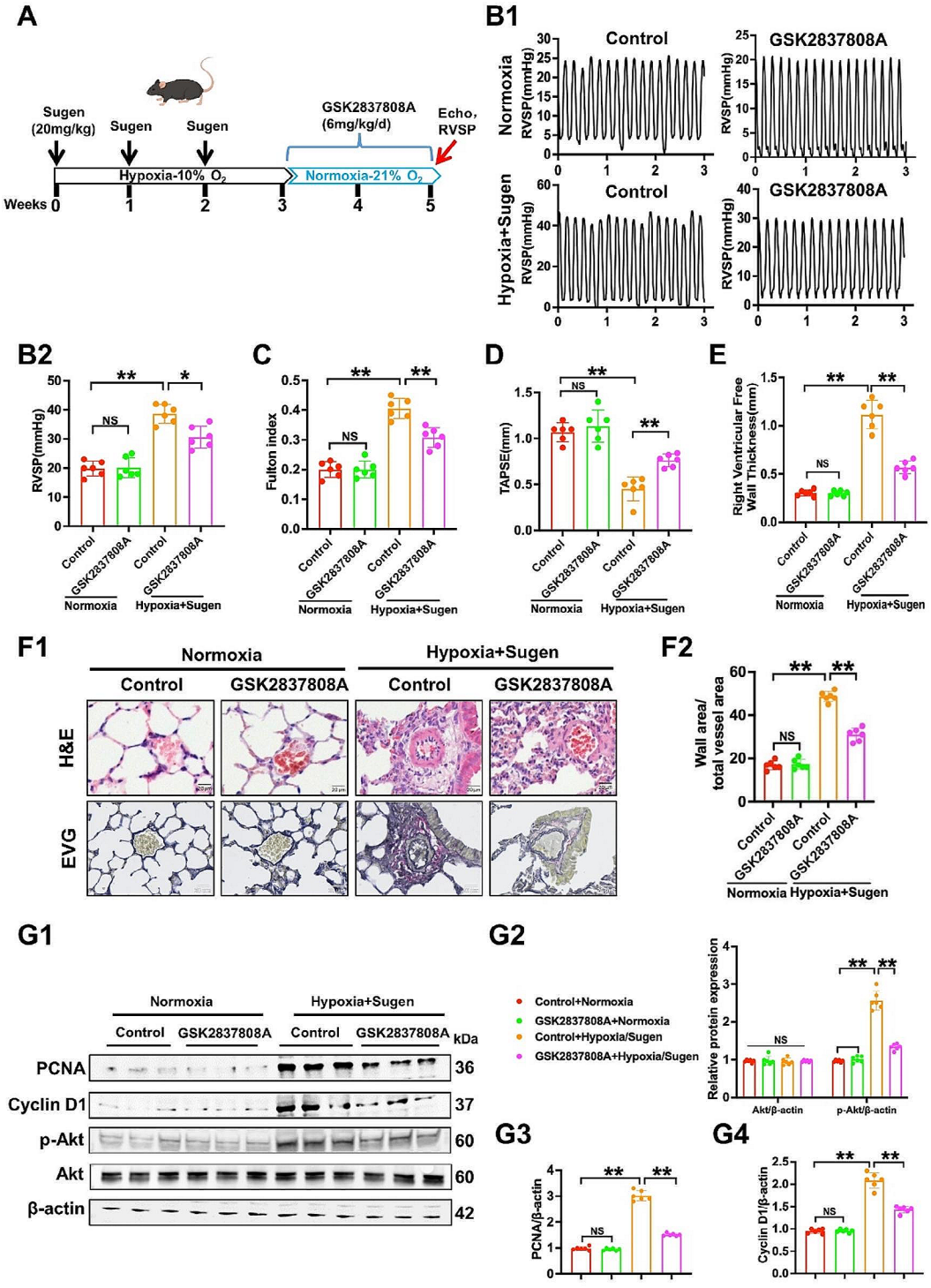

Fig. 6 Therapeutic effects of LDHA inhibitors in hypoxia/Sugen-induced pulmonary hypertension. (**A**) Illustration of the animal protocols. (**B to E**) The RVSP (B1, B2), Fulton index (**C**), TAPSE (**D**) and RVFWT (**E**) were determined in experimental mice with or without GSK2837808A treatment. (**F**) Representative histological images of lung sections stained with H&E and EVG in each experimental group (F1). The wall thickness of the pulmonary arteries was measured (F2). (**G**) Representative images of Western blots (G1) and the combined quantitative data show the expression of p-Akt, Akt (G2), PCNA (G3), Cyclin D1 (G4) of lung tissue in experimental groups. Data were presented as Mean ± SD. $n = 6$, NS: no statistical signification, $^{*}p < 0.05$, $^{**}p < 0.01$

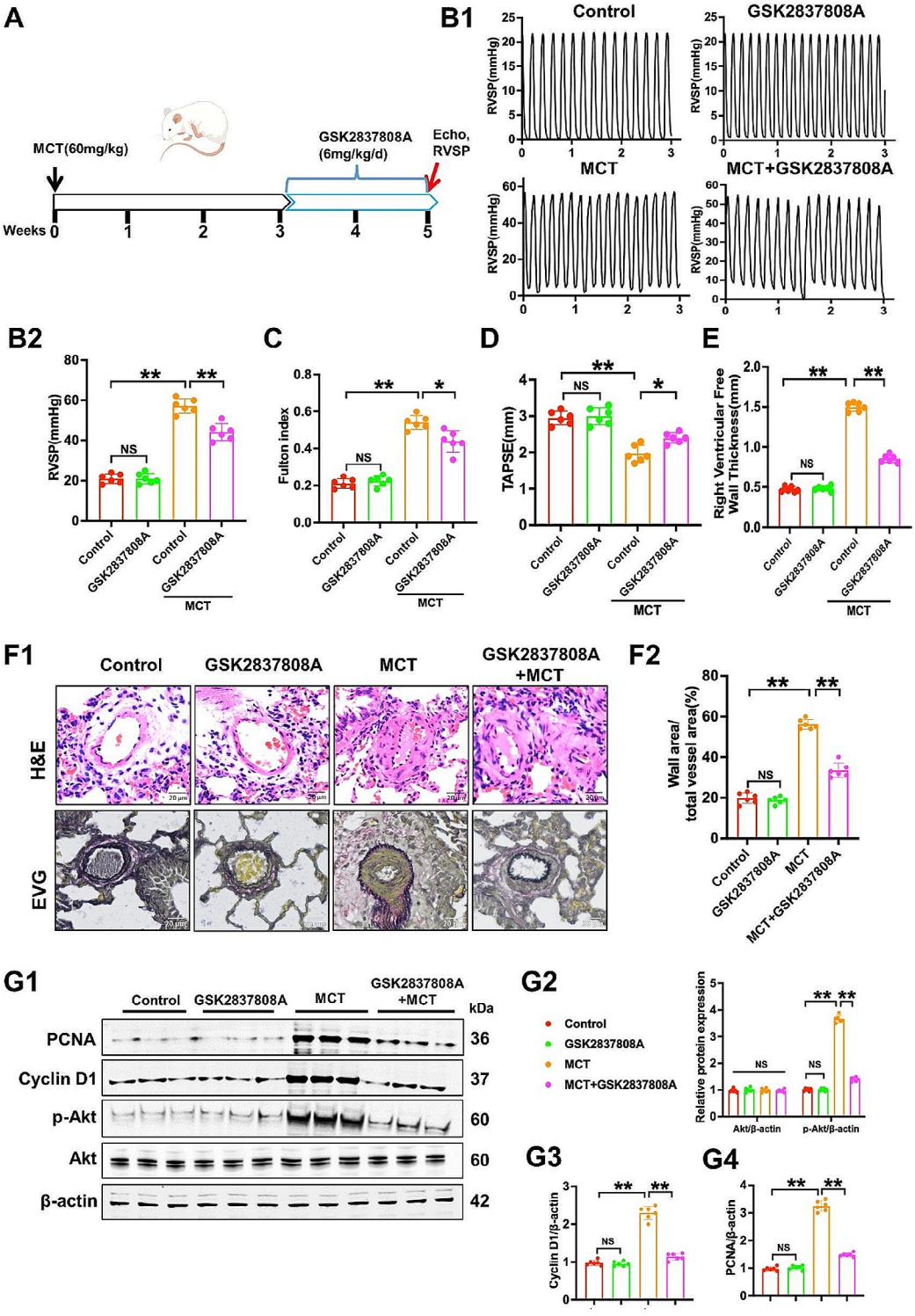

Fig. 7 Therapeutic effects of LDHA inhibitor in MCT-induced pulmonary hypertension. (**A**) Illustration of the animal protocols. (**B to E**) The RVSP (B1, B1), Fulton index (**C**), TAPSE (**D**) and RVFWT (**E**) were determined in experimental rats with or without GSK2837808A treatment. (**F**) Representative histological images of lung sections stained with H&E and EVG in each experimental group (F1). The wall thickness of the pulmonary arteries was measured (F2). (**G**) Representative images of Western blots (G1) and the combined quantitative data show the expression of p-Akt, Akt (G2), PCNA (G3), Cyclin D1 (G4) of lung tissue in experimental groups. Data were presented as Mean ± SD. $n = 6$, NS: no statistical signification, $^{*}p < 0.05$, $^{**}p < 0.01$

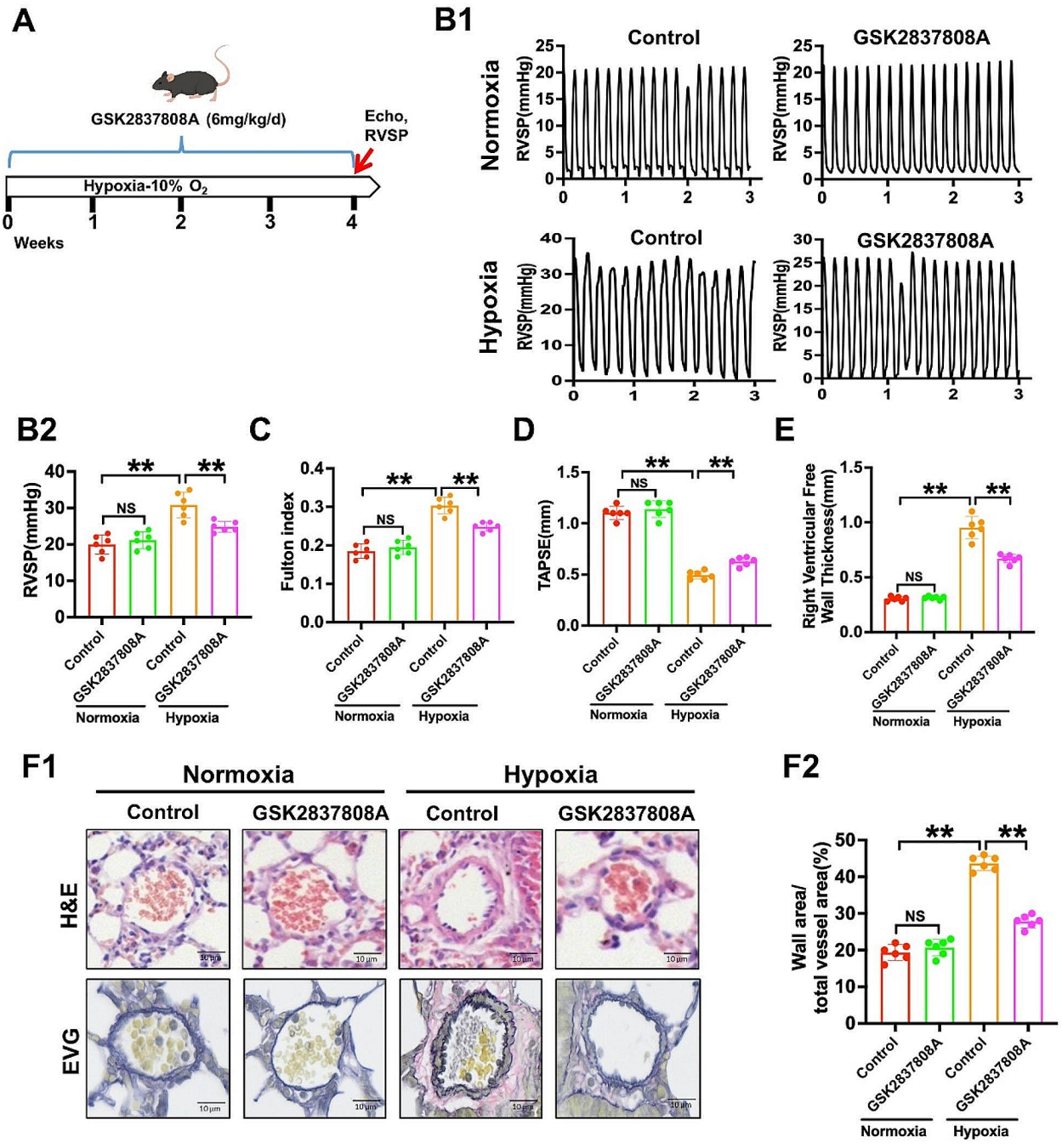

Fig. 8 Therapeutic effects of LDHA inhibitors in chronic hypoxia-induced mouse pulmonary hypertension. (**A**) Illustration of the animal protocols. (**B to E**) The RVSP (B1, B2), Fulton index (**C**), TAPSE (**D**) and RVFWT (**E**) were determined in experimental mice with or without GSK2837808A treatment. (**F**) Representative histological images of lung sections stained with H&E and EVG in each experimental group (F1). The wall thickness of the pulmonary arteries was measured (F2). Data were presented as Mean ± SD. $n = 6$, NS: no statistical signification, $^{*}p < 0.05$, $^{**}p < 0.01$

[36]. Furthermore, some evidence has also confirmed that lactate can promote the proliferation and metastasis of cancer cells [37]. Cancer and PH share many common pathological mechanisms [38]. This suggests that lactate may play an important role in PH. More importantly, the latest research indicates that hyperlactic acidemia is an independent predicting factor for the mortality of PH patients [7]. In this study, we found that lactate content in plasma and lung tissue were increased in mice exposed to hypoxia, and lactate promoted the proliferation and migration of PASMCs.

LDHA is a key metabolic enzyme that regulates lactate content in cells [39]. Similarly, LDHA plays an important role in a variety of cardiovascular diseases and tumors, being necessary for cell proliferation, growth and cell differentiation [40, 41]. This also indicates that the production and biological functions of lactate are mostly dependent on LDHA. It has been reported that PASMCs in PH exhibit excessive proliferation and migration. Multiple studies have suggested that inhibiting the proliferation and migration of PASMCs has a protective effect against PH [42, 43]. We found that LDHA was highly expressed in the PASMCs of mice with PH. Knockdown of LDHA in PASMCs significantly reduced the lactate content in plasma and lung tissue. Li Zhichao et al. showed that the lactate levels in the aorta and carotid arteries of mice with hypoxic PH did not significantly increase [44]. This also confirms that the lungs may be the main organs responsible for lactate production in mice with hypoxic PH and that lactate in the local microenvironment of the pulmonary artery may play a key role in vascular remodeling.

Metabolic reprogramming is a new hallmark of PH development [45]. Previous studies have confirmed that glycolysis is observed in PASMCs from patients with PH and in animal models [3]. Glycolysis can regulate the proliferation and migration of PASMCs [46]. In MCT-induced PH, PASMCs undergo glycolysis and promote vascular remodeling [46]; this indicates that glycolysis also exists in pulmonary artery smooth muscle cells in PH under normoxic conditions. Multiple studies have shown that key enzymes of glycolysis promote the proliferation and migration of PASMCs by promoting a metabolic shift towards glycolysis [47, 48]. Inhibiting glycolysis can reverse vascular remodeling in PH and reduce pulmonary artery pressure [49]. Previous studies have also confirmed that the overexpression of LDHA promotes glycolysis in tumor cells [19]. In this study, we found that knockdown of LDHA or an LHDA inhibitor can reduce pulmonary artery pressure and improve right ventricular function by attenuating pulmonary artery vascular re-modeling.

Akt is a key regulator of multiple metabolic enzymes and signaling pathways [50]. The PI3K-Akt signaling pathway regulates PASMCs proliferation and pulmonary arterial remodeling in PH [51]. Nie X et al. discovered that an Akt inhibitor attenuated pulmonary vascular remodeling in PH models [52]. In addition, previous studies have shown that lactate promotes tumor growth and metastasis by activating Akt [53]. Furthermore, Akt activation has been shown to contribute to glycolysis [54]. However, some studies have shown that lactate inhibits the Akt activation of macrophages and T cells [55]. We suggest that lactate may play different biological functions in different cells. Our results showed that Akt signaling activation was a potential pathway that mediated the role of LDHA/lactate in PASMC hyperproliferation. G protein-coupled receptor 81 (GPR81) serves as an endogenous receptor for lactate, and previous studies have shown that extracellular lactate can activate the PI3K-Akt signaling pathway through GPR81 [56]. Our study has demonstrated that lactate activates the Akt signaling pathway to promote PASMCs proliferation. However, whether GPR81 acts as a lactate receptor and mediates this process was not investigated. This aspect merits further exploration in future studies [57]. In addition, lactate enters cells through Monocarboxylate transporter-1 (MCT1) [58]. Research has shown that lactate can promote an increase in MCT1 expression, and MCT1 plays an important role in cancer cell proliferation and migration [59]. Recent evidence has shown that lactate plays an important role in the post-translational modification of proteins, and it has been reported that the modification of histones by lactate occurs in pulmonary artery smooth muscle cells in PH [60]. The latest reports indicate that intracellular lactate can directly regulate protein function to control cell cycles and proliferation [61]. Furthermore, Xin Cai et al. found that lactate can directly enter mitochondria and activate the respiratory chain to increase mitochondrial ATP production [62]. Recently, Sun et al. reported that lactate promotes lung fibrosis by increasing mitochondrial fission-derived ROS via the ERK/DRP1 signaling pathway [63]. Additionally, the ERK1/2/DRP1 signaling pathway has been shown to mediate HMGB1-induced PH development [64]. These studies suggest that lactate may influence PASMCs proliferation through the ERK/DRP1 pathway and mitochondrial fission. Therefore, the specific mechanism by which lactate promotes the proliferation of PASMCs deserves further study.

This study has certain limitations. First, to reduce experimental variability, only male animals were used to establish the PH model. Female animals should be included in future studies to ensure comprehensive evaluation. Second, there was a lack of conditional knockout mice with LDHA smooth muscle cells included in this study. Third, we did not investigate the specific mechanism by which lactate activates Akt. Finally, we used a hypoxic mouse model to examine the impact of lactate

and LDHA on PH, further validation in hypoxia-induced rat PH models is necessary in future research. We remain committed to enhancing our understanding of lactate and its role in promoting vascular remodeling in PH in future investigations.

Conclusion

In summary, this study shows that high LDHA expression contributes to hypoxia-induced lactate production and promotes PH vascular remodeling and right ventricular remodeling. Activation of the Akt signaling pathway is regulated by LDHA/lactate and leads to a high proliferation phenotype of PASMCs. Inhibitors of LDHA can partially reverse pulmonary arterial hypertension vascular remodeling and improve right heart function. This study provides a new molecular target for the development of new treatments for PH.

Abbreviations

EVG	Elastica Van Gieson
GPR81	G protein-coupled receptor 81
H&E	Hematoxylin-Eosin
LDHA	Lactate dehydrogenase A
LV	Left Ventricle
MCT	Monocrotaline
MCT1	Monocarboxylate Transporter-1
PAT	Pulmonary Acceleration Time
PASMCs	Pulmonary Artery Smooth Muscle Cells
PET	Pulmonary Ejection Time
PH	Pulmonary Hypertension
TAPSE	Tricuspid Annular Plane Systolic Excursion
RV	Right Ventricular
RVFAC	Right Ventricular Fractional Area Change
RVFWT	Right Ventricular Free Wall Thickness
RVSP	Right Ventricular Systolic Pressures
S	Septum
SuHx	Sugen/hypoxia

Supplementary Information

The online version contains supplementary material available at https://doi.org/10.1186/s12967-024-05543-7.

Supplementary Material 1

Acknowledgements

We thank Yu Han, Ming Tang for their technical assistance.

Author contributions

XBL conceived the idea, designed the study, and supervised all experiments. DQW and SW performed the experiments, analyzed the data, and wrote the original draft of the paper. FXW and QZ participated in the validation of experiments and visualization of results. ZZ revised the manuscript. All authors approved the final manuscript.

Funding

This work was supported by grants from Chongqing scientific research institutions performance incentive and guidance project (cstc2022jxjl120028), Sichuan Science and Technology Program (2024NSFSC1717) and The Third People's Hospital of Chengdu Clinical Research Program (CSY-YN-01-2023-040).

Data availability

The data that support the findings of this study are available from the corresponding author upon reasonable request.

Declarations

Institutional review board statement

The animal study protocol was approved by the Institutional Review Board of Third Military Medical University Animal Care and Use Committee (AMUWEC20201184).

Consent for publication

All authors have agreed to the content of the manuscript and agree to this submission.

Competing interests

All authors declare no conflict of interest.

Received: 28 May 2024 / Accepted: 26 July 2024
Published online: 05 August 2024

References

1. Ruopp NF, Cockrill BA. Diagnosis and treatment of pulmonary arterial hypertension: a review. JAMA. 2022;327(14):1379–91.
2. Thenappan T, Ormiston ML, Ryan JJ, Archer SL. Pulmonary arterial hypertension: pathogenesis and clinical management. BMJ. 2018;360:j5492.
3. Li D, Shao NY, Moonen JR, Zhao Z, Shi M, Otsuki S, Wang L, Nguyen T, Yan E, Marciano DP, Contrepois K, Li CG, Wu JC, Snyder MP, Rabinovitch M. ALDH1A3 coordinates metabolism with Gene Regulation in Pulmonary arterial hypertension. Circulation. 2021;143(21):2074–90.
4. Chen J, Zhu Y, Wu C, Shi J. Engineering lactate-modulating nanomedicines for cancer therapy. Chem Soc Rev. 2023;52(3):973–1000.
5. Xu W, Janocha AJ, Erzurum SC. Metabolism in Pulmonary Hypertension. Annu Rev Physiol. 2021;83:551–76.
6. Piper B, Bogamuwa S, Hossain T, Farkas D, Rosas L, Green AC, Newcomb G, Sun N, Ovando-Ricardez JA, Horowitz JC, Bhagwani AR, Yang H, Kudryashova TV, Rojas M, Mora AL, Yan P, Mallampalli RK, Goncharova EA, Eckmann DM, Farkas L. RAB7 deficiency impairs pulmonary artery endothelial function and promotes pulmonary hypertension. J Clin Invest. 2024;134(3):e169441.
7. Deng X, Jiang N, Huang C, Zhou S, Peng L, Zhang L, Liu J, Wang L, Zhou J, Wang Q, Weng L, Peng J, Zhao J, Li M, Zeng X. Mortality and prognostic factors in connective tissue disease-associated pulmonary arterial hypertension patients complicated with right heart failure. Int J Rheum Dis. 2023;26(5):862–9.
8. Ye L, Jiang Y, Zhang M. Crosstalk between glucose metabolism, lactate production and immune response modulation. Cytokine Growth Factor Rev. 2022;68:81–92.
9. Kim S, Park DH, Lee SH, Kwak HB, Kang JH. Contribution of high-intensity interval Exercise in the fasted state to Fat Browning: potential roles of Lactate and β-Hydroxybutyrate. Med Sci Sports Exerc. 2023;55(7):1160–71.
10. Chen Y, Wu J, Zhai L, Zhang T, Yin H, Gao H, Zhao F, Wang Z, Yang X, Jin M, Huang B, Ding X, Li R, Yang J, He Y, Wang Q, Wang W, Kloeber JA, Li Y, Hao B, Zhang Y, Wang J, Tan M, Li K, Wang P, Lou Z, Yuan J. Metabolic regulation of homologous recombination repair by MRE11 lactylation. Cell. 2024;187(2):294–e31121.
11. Han X, Du S, Chen X, Min X, Dong Z, Wang Y, Zhu C, Wei F, Gao S, Cai Q. Lactate-mediated fascin protrusions promote cell adhesion and migration in cervical cancer. Theranostics. 2023;13(7):2368–83.
12. Lin J, Liu G, Chen L, Kwok HF, Lin Y. Targeting lactate-related cell cycle activities for cancer therapy. Semin Cancer Biol. 2022;86(Pt 3):1231–43.
13. Urbańska K, Orzechowski A. Unappreciated role of LDHA and LDHB to Control Apoptosis and autophagy in Tumor cells. Int J Mol Sci. 2019;20(9):2085.
14. Masson B, Le Ribeuz H, Sabourin J, Laubry L, Woodhouse E, Foster R, Ruchon Y, Dutheil M, Boët A, Ghigna MR, De Montpreville VT, Mercier O, Beech DJ, Benitah JP, Bailey MA, Humbert M, Montani D, Capuano V, Antigny F. Orai1 inhibitors as potential treatments for pulmonary arterial hypertension. Circ Res. 2022;131(9):e102–19.
15. Feng Y, Xiong Y, Qiao T, Li X, Jia L, Han Y. Lactate dehydrogenase A: a key player in carcinogenesis and potential target in cancer therapy. Cancer Med. 2018;7(12):6124–36.
16. Vlasiou M, Nicolaidou V, Papaneophytou C. Targeting Lactate Dehydrogenase-B as a strategy to Fight Cancer: identification of potential inhibitors by in Silico Analysis and in Vitro Screening. Pharmaceutics. 2023;15(10):2411.

17. An YJ, Jo S, Kim JM, Kim HS, Kim HY, Jeon SM, Han D, Yook JI, Kang KW, Park S. Lactate as a major epigenetic carbon source for histone acetylation via nuclear LDH metabolism. Exp Mol Med. 2023;55(10):2238–47.
18. Huo N, Cong R, Sun ZJ, Li WC, Zhu X, Xue CY, Chen Z, Ma LY, Chu Z, Han YC, Kang XF, Jia SH, Du N, Kang L, Xu XJ. STAT3/LINC00671 axis regulates papillary thyroid tumor growth and metastasis via LDHA-mediated glycolysis. Cell Death Dis. 2021;12(9):799.
19. Wu C, Zheng C, Chen S, He Z, Hua H, Sun C, Yu C. FOXQ1 promotes pancreatic cancer cell proliferation, tumor stemness, invasion and metastasis through regulation of LDHA-mediated aerobic glycolysis. Cell Death Dis. 2023;14(10):699.
20. Chen Y, Wu G, Li M, Hesse M, Ma Y, Chen W, Huang H, Liu Y, Xu W, Tang Y, Zheng H, Li C, Lin Z, Chen G, Liao W, Liao Y, Bin J, Chen Y. LDHA-mediated metabolic reprogramming promoted cardiomyocyte proliferation by alleviating ROS and inducing M2 macrophage polarization. Redox Biol. 2022;56:102446.
21. Dai C, Li Q, May HI, Li C, Zhang G, Sharma G, Sherry AD, Malloy CR, Khemtong C, Zhang Y, Deng Y, Gillette TG, Xu J, Scadden DT, Wang ZV. Lactate Dehydrogenase A governs Cardiac Hypertrophic Growth in response to hemodynamic stress. Cell Rep. 2020;32(9):108087.
22. Dahoui HA, Hayek MN, Nietert PJ, Arabi MT, Muwakkit SA, Saab RH, Bissar AN, Jumaa NM, Farhat FS, Dabbous IA, Bitar FF, Abboud MR. Pulmonary hypertension in children and young adults with sickle cell disease: evidence for familial clustering. Pediatr Blood Cancer. 2010;54(3):398–402.
23. Lüscher TF. Pulmonary hypertension, gender issues, and quality of care. Eur Heart J. 2016;37(1):1–3.
24. Philip JL, Tabima DM, Wolf GD, Frump AL, Cheng TC, Schreier DA, Hacker TA, Lahm T, Chesler NC. Exogenous estrogen preserves distal pulmonary arterial mechanics and prevents pulmonary hypertension in rats. Am J Respir Crit Care Med. 2020;201(3):371–4.
25. Hester J, Ventetuolo C, Lahm T, Sex. Gender, and sex hormones in pulmonary hypertension and right ventricular failure. Compr Physiol. 2019;10(1):125–70.
26. Hu S, Wang L, Xu Y, Li F, Wang T. Disulfiram attenuates hypoxia-induced pulmonary hypertension by inhibiting GSDMD cleavage and pyroptosis in HPASMCs. Respir Res. 2022;23(1):353.
27. Gupta VK, Sharma NS, Durden B, Garrido VT, Kesh K, Edwards D, Wang D, Myer C, Mateo-Victoriano B, Kollala SS, Ban Y, Gao Z, Bhattacharya SK, Saluja A, Singh PK, Banerjee S. Hypoxia-driven Oncometabolite L-2HG maintains stemness-differentiation balance and facilitates Immune Evasion in Pancreatic Cancer. Cancer Res. 2021;81(15):4001–13.
28. Zhu Z, Wang Y, Long A, Feng T, Ocampo M, Chen S, Tang H, Guo Q, Minshall R, Makino A, Huang W, Chen J. Pulmonary vessel casting in a rat model of monocrotaline-mediated pulmonary hypertension. Pulm Circ. 2020;10(3):2045894020922129.
29. Li X, Zhang Z, Luo M, Cheng Z, Wang R, Liu Q, Lv D, Yan J, Shang F, Luo S, Xia Y. NLRP3 inflammasome contributes to endothelial dysfunction in angiotensin II-induced hypertension in mice. Microvasc Res. 2022;143:104384.
30. Miro C, Di Cicco E, Ambrosio R, Mancino G, Di Girolamo D, Cicatiello AG, Sagliocchi S, Nappi A, De Stefano MA, Luongo C, Antonini D, Visconte F, Varricchio S, Ilardi G, Del Vecchio L, Staibano S, Boelen A, Blanpain C, Missero C, Salvatore D, Dentice M. Thyroid hormone induces progression and invasiveness of squamous cell carcinomas by promoting a ZEB-1/E-cadherin switch. Nat Commun. 2019;10(1):5410.
31. Pan Q, Xie X, Yuan Q. Monocarboxylate transporter 4 protects against myocardial ischemia/reperfusion injury by inducing oxidative phosphorylation/glycolysis interconversion and inhibiting oxidative stress. Clin Exp Pharmacol Physiol. 2023;50(12):954–63.
32. Zhu Y, Wu F, Hu J, Xu Y, Zhang J, Li Y, Lin Y, Liu X. LDHA deficiency inhibits trophoblast proliferation via the PI3K/AKT/FOXO1/CyclinD1 signaling pathway in unexplained recurrent spontaneous abortion. FASEB J. 2023;37(2):e22744.
33. Xu R, Yuan W, Wang Z. Advances in glycolysis metabolism of atherosclerosis. J Cardiovasc Transl Res. 2023;16(2):476–90.
34. Zhang N, Zhang Y, Xu J, Wang P, Wu B, Lu S, Lu X, You S, Huang X, Li M, Zou Y, Liu M, Zhao Y, Sun G, Wang W, Geng D, Liu J, Cao L, Sun Y. α-myosin heavy chain lactylation maintains sarcomeric structure and function and alleviates the development of heart failure. Cell Res. 2023;33(9):679–98.
35. Zhou J, Sun L, Chen L, Liu S, Zhong L, Cui M. Comprehensive metabolomic and proteomic analyses reveal candidate biomarkers and related metabolic networks in atrial fibrillation. Metabolomics. 2019;15(7):96.
36. Yang L, Gao L, Nickel T, Yang J, Zhou J, Gilbertsen A, Geng Z, Johnson C, Young B, Henke C, Gourley GR, Zhang J. Lactate promotes synthetic phenotype in vascular smooth muscle cells. Circ Res. 2017;121(11):1251–62.
37. Bo W, Yu N, Wang X, Wang C, Liu C. Lactate promoted cisplatin resistance in NSCLC by modulating the m6A modification-mediated FOXO3/MAGI1-IT1/miR-664b-3p/IL-6R axis. Neoplasia. 2024;48:100960.
38. Price LC, Seckl MJ, Dorfmüller P, Wort SJ. Tumoral pulmonary hypertension. Eur Respir Rev. 2019;28(151):180065.
39. Chen M, Cen K, Song Y, Zhang X, Liou YC, Liu P, Huang J, Ruan J, He J, Ye W, Wang T, Huang X, Yang J, Jia Y, Liang X, Shen P, Wang Q, Liang T. NUSAP1-LDHA-Glycolysis-lactate feedforward loop promotes Warburg effect and metastasis in pancreatic ductal adenocarcinoma. Cancer Lett. 2023;567:216285.
40. Fan M, Yang K, Wang X, Chen L, Gill PS, Ha T, Liu L, Lewis NH, Williams DL, Li C. Lactate promotes endothelial-to-mesenchymal transition via Snail1 lactylation after myocardial infarction. Sci Adv. 2023;9(5):eadc9465.
41. Juraschek SP, Bower JK, Selvin E, Subash Shantha GP, Hoogeveen RC, Ballantyne CM, Young JH. Plasma lactate and incident hypertension in the atherosclerosis risk in communities study. Am J Hypertens. 2015;28(2):216–24.
42. Ma Q, Yang Q, Xu J, Sellers HG, Brown ZL, Liu Z, Bordan Z, Shi X, Zhao D, Cai Y, Pareek V, Zhang C, Wu G, Dong Z, Verin AD, Gan L, Du Q, Benkovic SJ, Xu S, Asara JM, Ben-Sahra I, Barman S, Su Y, Fulton DJR, Huo Y. Purine synthesis suppression reduces the development and progression of pulmonary hypertension in rodent models. Eur Heart J. 2023;44(14):1265–79.
43. Ruffenach G, Medzikovic L, Aryan L, Li M, Eghbali M. HNRNPA2B1: RNA-Binding protein that orchestrates smooth muscle cell phenotype in pulmonary arterial hypertension. Circulation. 2022;146(16):1243–58.
44. Chen J, Zhang M, Liu Y, Zhao S, Wang Y, Wang M, Niu W, Jin F, Li Z. Histone lactylation driven by mROS-mediated glycolytic shift promotes hypoxic pulmonary hypertension. J Mol Cell Biol. 2023;14(12):mjac073.
45. Huang YZ, Wu JC, Lu GF, Li HB, Lai SM, Lin YC, Gui LX, Sham JSK, Lin MJ, Lin DC. Pulmonary hypertension induces serotonin hyperreactivity and metabolic reprogramming in coronary arteries via NOX1/4-TRPM2 signaling pathway. Hypertension. 2024;81(3):582–94.
46. Rafikova O, Meadows ML, Kinchen JM, Mohney RP, Maltepe E, Desai AA, Yuan JX, Garcia JG, Fineman JR, Rafikov R, Black SM. Metabolic changes precede the development of Pulmonary Hypertension in the Monocrotaline exposed rat lung. PLoS ONE. 2016;11(3):e0150480.
47. Zhang C, Sun Y, Guo Y, Xu J, Zhao H. JMJD1C promotes smooth muscle cell proliferation by activating glycolysis in pulmonary arterial hypertension. Cell Death Discov. 2023;9(1):98.
48. Kovacs L, Cao Y, Han W, Meadows L, Kovacs-Kasa A, Kondrikov D, Verin AD, Barman SA, Dong Z, Huo Y, Su Y. PFKFB3 in smooth muscle promotes vascular remodeling in pulmonary arterial hypertension. Am J Respir Crit Care Med. 2019;200(5):617–27.
49. Li W, Chen W, Peng H, Xiao Z, Liu J, Zeng Y, Huang T, Song Q, Wang X, Xiao Y. Shikonin improves pulmonary vascular remodeling in monocrotaline–induced pulmonary arterial hypertension via regulation of PKM2. Mol Med Rep. 2023;27(3):60.
50. Liu R, Chen Y, Liu G, Li C, Song Y, Cao Z, Li W, Hu J, Lu C, Liu Y. PI3K/AKT pathway as a key link modulates the multidrug resistance of cancers. Cell Death Dis. 2020;11(9):797.
51. Shi Y, Liu J, Zhang R, Zhang M, Cui H, Wang L, Cui Y, Wang W, Sun Y, Wang C. Targeting endothelial ENO1 (Alpha-Enolase) -PI3K-Akt-mTOR Axis alleviates hypoxic pulmonary hypertension. Hypertension. 2023;80(5):1035–47.
52. Nie X, Wu Z, Shang J, Zhu L, Liu Y, Qi Y. Curcumol suppresses endothelial-to-mesenchymal transition via inhibiting the AKT/GSK3β signaling pathway and alleviates pulmonary arterial hypertension in rats. Eur J Pharmacol. 2023;943:175546.
53. Wang L, Li S, Luo H, Lu Q, Yu S. PCSK9 promotes the progression and metastasis of colon cancer cells through regulation of EMT and PI3K/AKT signaling in tumor cells and phenotypic polarization of macrophages. J Exp Clin Cancer Res. 2022;41(1):303.
54. Pan T, Sun S, Chen Y, Tian R, Chen E, Tan R, Wang X, Liu Z, Liu J, Qu H. Immune effects of PI3K/Akt/HIF-1α-regulated glycolysis in polymorphonuclear neutrophils during sepsis. Crit Care. 2022;26(1):29.
55. Zhang W, Wang G, Xu ZG, Tu H, Hu F, Dai J, Chang Y, Chen Y, Lu Y, Zeng H, Cai Z, Han F, Xu C, Jin G, Sun L, Pan BS, Lai SW, Hsu CC, Xu J, Chen ZZ, Li HY, Seth P, Hu J, Zhang X, Li H, Lin HK. Lactate is a natural suppressor of RLR Signaling by Targeting MAVS. Cell. 2019;178(1):176–e18915.
56. Wu Y, Wang M, Zhang K, Li Y, Xu M, Tang S, Qu X, Li C. Lactate enhanced the effect of parathyroid hormone on osteoblast differentiation via GPR81-PKC-Akt signaling. Biochem Biophys Res Commun. 2018;503(2):737–43.

57. Wu P, Zhu T, Huang Y, Fang Z, Luo F. Current understanding of the contribution of lactate to the cardiovascular system and its therapeutic relevance. Front Endocrinol (Lausanne). 2023;14:1205442.
58. Zhao Y, Li M, Yao X, Fei Y, Lin Z, Li Z, Cai K, Zhao Y, Luo Z. HCAR1/MCT1 regulates Tumor Ferroptosis through the lactate-mediated AMPK-SCD1 activity and its therapeutic implications. Cell Rep. 2020;33(10):108487.
59. Fan Q, Yang L, Zhang X, Ma Y, Li Y, Dong L, Zong Z, Hua X, Su D, Li H, Liu J. Autophagy promotes metastasis and glycolysis by upregulating MCT1 expression and Wnt/β-catenin signaling pathway activation in hepatocellular carcinoma cells. J Exp Clin Cancer Res. 2018;37(1):9.
60. Zhao SS, Liu J, Wu QC, Zhou XL. Role of histone lactylation interference RNA m6A modification and immune microenvironment homeostasis in pulmonary arterial hypertension. Front Cell Dev Biol. 2023;11:1268646.
61. Liu W, Wang Y, Bozi LHM, Fischer PD, Jedrychowski MP, Xiao H, Wu T, Darabedian N, He X, Mills EL, Burger N, Shin S, Reddy A, Sprenger HG, Tran N, Winther S, Hinshaw SM, Shen J, Seo HS, Song K, Xu AZ, Sebastian L, Zhao JJ, Dhe-Paganon S, Che J, Gygi SP, Arthanari H, Chouchani ET. Lactate regulates cell cycle by remodelling the anaphase promoting complex. Nature. 2023;616(7958):790–7.
62. Cai X, Ng CP, Jones O, Fung TS, Ryu KW, Li D, Thompson CB. Lactate activates the mitochondrial electron transport chain independently of its metabolism. Mol Cell. 2023;83(21):3904–e39207.
63. Sun Z, Ji Z, Meng H, He W, Li B, Pan X, Zhou Y, Yu G. Lactate facilitated mitochondrial fission-derived ROS to promote pulmonary fibrosis via ERK/DRP-1 signaling. J Transl Med. 2024;22(1):479.
64. Feng W, Wang J, Yan X, Zhang Q, Chai L, Wang Q, Shi W, Chen Y, Liu J, Qu Z, Li S, Xie X, Li M. ERK/Drp1-dependent mitochondrial fission contributes to HMGB1-induced autophagy in pulmonary arterial hypertension. Cell Prolif. 2021;54(6):e13048.

Publisher's Note